Bending fatigue characteristics of a reinforced macadam base

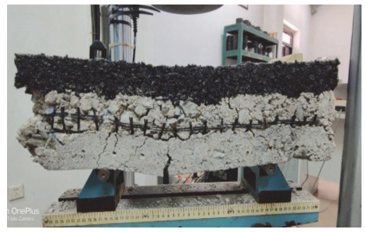

Características de fatiga por flexión de una base de macadán reforzada

Hongjun Jing[1,2*], Xiangyu Chen[1,2], Yunliang Zhang[3], Guoping Zhang[4] and Binhui Ren[5]

[1] School of Civil and Architectural Engineering, Xi'an University of Science and Technology – 710054 Xi'an Shaanxi (China).
[2] Road Engineering Research Center. Xi'an University of Science and Technology – 710054 Xi'an Shaanxi (China).
[3] SCEGC No.3 Construction Engineering Group Company Ltd. - 710054 Xi'an (China).
[4] Rural Road Maintenance Center of Yuyang District – 719099 Yulin (China).
[5] Highway Administration of Yulin - 719054 Yulin (China).

DOI: https://doi.org/10.52152/D11402 | Received: 02/jan/2025 • Reviewing: 05/jan/2025 • Accepted: 25/mar/2025

To cite this article: JING, Hongjun; CHEN, Xiangyu; ZHANG, Xiangyu; ZHANG, Xiangyu; REN, Binhui. BENDING FATIGUE CHARACTERISTICS OF REINFORCED MACADAM BASE. *DYNA* July August 2025. Vol. 100, n.4, pp. 350-356. DOI: https://doi.org/10.52152/D11402

RESUMEN

- La estructura de base de macadam tradicional presenta una baja resistencia a la deformación por flexión de la carretera. Sin embargo, los métodos de refuerzo para mejorar el rendimiento de las estructuras de base de macadam no han sido completamente explorados. En particular, aún faltan técnicas efectivas para mejorar el comportamiento a flexión y la vida útil a fatiga de las estructuras de base flexibles. En este estudio, se propuso el uso de geomallas para reforzar las estructuras de base de macadam. Se llevaron a cabo pruebas exhaustivas para evaluar el desempeño a flexión y la resistencia a la fatiga de especímenes reforzados y no reforzados. Estas pruebas incluyeron ensayos de resistencia a tracción por flexión, ensayos de fatiga en flexión en tres puntos y ensayos de carga cíclica aplicados en cinco niveles de esfuerzo distintos. Los resultados muestran que las bases de macadam no reforzadas presentan un bajo rendimiento a flexión. Cuando la carga alcanza el nivel de esfuerzo de 0.8, los especímenes no reforzados experimentan falla por fatiga de bajo ciclo, caracterizada por un pequeño desplazamiento último y un plano de falla claramente definido. Con la incorporación del refuerzo de geomalla, la vida útil a fatiga de los especímenes mejora significativamente, sin un deterioro notable en las curvas de esfuerzo-deformación incluso en niveles de carga elevados. Los especímenes reforzados mantienen un comportamiento de fatiga de alto ciclo en el nivel de esfuerzo de 0.8, evitando así la falla por fatiga de bajo ciclo. Además, los especímenes reforzados suprimen eficazmente la propagación de **grietas por reflexión** en el centro del tramo de la base de piedra triturada estabilizada con cemento y retrasan la extensión de grietas de corte diagonal cerca de los apoyos, mejorando así significativamente la estabilidad dinámica y la durabilidad a largo plazo de la capa de base de piedra triturada en las estructuras de pavimento. Estos hallazgos proporcionan una referencia teórica para la aplicación práctica de esta tecnología de refuerzo en estructuras de base de macadam.
- **Palabras clave:** ingeniería de carreteras, base de macadam reforzada, ensayo de fatiga por flexión, rendimiento a fatiga por flexión, geomalla.

ABSTRACT

The traditional macadam base structure has poor resistance to road bending deformation. However, reinforcement methods to improve the performance of macadam base structures have not been fully explored. In particular, effective techniques to enhance the bending performance and fatigue life of flexible base structures are still lacking. In this study, geogrids were proposed to reinforce macadam base structures. Comprehensive tests were conducted to evaluate the bending performance and fatigue resistance of reinforced and unreinforced specimens. These tests included bending tensile strength tests, three-point bending fatigue tests, and cyclic loading tests applied at five distinct stress levels. The results show that unreinforced macadam bases have poor bending performance. When the load reaches the 0.8 stress level, the unreinforced specimens experience low-cycle fatigue failure, characterized by a small ultimate displacement and a distinct failure plane. With the inclusion of geogrid reinforcement, the fatigue life of the specimens is significantly improved, with no notable deterioration in the stress-strain yield curves even at high load levels. Reinforced specimens maintain high-cycle fatigue performance at the 0.8 stress level, thereby avoiding low-cycle fatigue failure. Furthermore, the reinforced specimens effectively suppress the propagation of mid-span reflective cracks in the cement-stabilized crushed stone base and delay the extension of diagonal shear cracks near the supports, thereby significantly improving the dynamic stability and long-term durability of the crushed stone base layer in the pavement structures. These findings provide a theoretical reference for the practical application of this reinforcement technology in macadam base structures.

Keywords: highway engineering, reinforced macadam base, bending fatigue test, bending fatigue performance; geogrid.

1. INTRODUCTION

Advancements in composite pavement base structures have led to widespread use of geogrid reinforcement in subgrade engineering. Geogrids are placed between the semirigid base and asphalt surface to reduce flexural cracks. However, the high stiffness of traditional semirigid bases limits their ability to control reflection crack formation and propagation. Even with geogrid reinforcement, the inherent limitations of the semirigid base may prevent optimal performance. To address reflection cracks and improve base durability, we propose a simple, easily constructed composite-reinforced macadam base structure, which enhances road durability and dynamic stability.

Traditional semirigid bases are prone to significant reflection cracks, and various reinforcement methods have been extensively studied by scholars [1]–[4]. The dynamic stability of pavements can be effectively enhanced through geogrid reinforcement, which involves the influence of reinforcing material properties on the reinforcement effectiveness [5]–[7] and theoretical calculation models for reinforcement [8]–[11]. Full-scale laboratory fatigue tests have also been conducted to examine the reflection cracking of pavements [12]–[14]. Challenges such as high testing costs, limited sample sizes, and human errors hinder the ability to fully capture the behavior of reinforced composite base structures. As flexible base structures evolve, innovative anti-cracking solutions like macadam anti-crack buffer layers have emerged. While these structures improve crack resistance, they suffer from low stiffness, loose configurations, and lack of cementation, making them more prone to bending failure under fatigue loading, especially with subgrade subsidence and sub-base separation. The bending fatigue performance of macadam bases is still underexplored, and no effective methods have been proposed to enhance it. This study aims to improve the bending fatigue performance of composite macadam base structures by reinforcing them with geogrids and conducting three-point bending fatigue tests to investigate their bending failure and fatigue behavior.

2. STATE OF THE ART

As a new type of anti-crack structures, flexible macadam bases have garnered significant attention over the years. They are characterized by a loose structure and a lack of cementation, with the vehicle load on the structural layer offset by the rearrangement of particles. Existing literature indicates that the material properties and anti-cracking effectiveness of flexible macadam stress-absorbing layers have been analyzed through numerical simulations and laboratory experiments. Several design methods suitable for engineering applications have also been proposed.

Numerous studies have shown that flexible anti-crack buffer layers are ineffective in controlling bending fatigue cracks and extending the service life of pavement base structures under various loads. Additionally, the bending fatigue performance of these layers has been insufficiently evaluated. To enhance base structure performance, several researchers have proposed geogrid-based reinforcement, which has been tested in laboratories for effectiveness. Gonzalez Torre et al. [15] conducted a comparative study on the anticracking effects of six types of geosynthetic materials through indoor tests, revealing that geogrids outperformed geotextiles in terms of reflection crack resistance, particularly those with high secant modulus values, which provided the best performance against reflection cracks. Similarly, Saha et al. [16] carried out a series of indoor model tests on unreinforced and reinforced wet macadam mixtures to investigate their settlement characteristics, confirming that the bearing capacity of reinforced wet macadam mixtures was significantly enhanced.

Saride et al. [17] studied the role of geogrids in reducing reflection cracks and improving the fatigue performance of asphalt overlays using bending fatigue tests and digital image correlation. They found that geogrids with high shear and tensile bonding properties effectively inhibited reflection cracks and extended overlay fatigue life. Correia et al. [18] used a cyclic wheel load device to test geogrid-reinforced flexible pavements, showing that geogrids enhanced structural performance and reduced surface tracking and lateral displacement. Hadi et al. [19] examined the reinforcement effect of geogrids on concrete pavement fatigue and proposed a fatigue equation for pavements under cyclic loads. These studies demonstrate that geogrid-reinforced macadam bases improve structural performance and prevent reflection cracks, rutting, and displacement. However, a dynamic analysis of 3D anisotropic multilayer pavements under vehicle loads is lacking, along with comprehensive performance evaluations and comparative studies. To address this, this study conducted three-point bending fatigue tests, bending tensile tests, and cyclic load tests on reinforced and unreinforced base structures under five stress levels, analyzing changes in bending fatigue performance. When evaluating crack resistance in macadam bases, both material properties and engineering calculation methods should be considered. Valli et al. [20] studied the effects of natural rubber, carbon black, and copper slag on flexible base structures. They found that natural rubber improved vibration absorption, while copper slag enhanced the mechanical properties of the mixture. Carbon black increased tear strength, conductivity, and elasticity of asphalt. Patil et al. [21] improved backfill soil quality in India by adding a powdered inorganic admixture, which, after 7 days of curing, formed a flexible base structure. Habbouche et al. [22] proposed using a buffer layer to alleviate reflection cracks in asphalt coatings, which was validated through field tests. While these materials offer benefits for flexible bases, their performance under varying conditions has not been thoroughly explored, potentially affecting the fundamental properties of flexible bases. Future research should evaluate base structure performance under different conditions. You et al. [23] introduced an analytical method using Fourier waveform-combined changes to analyze the dynamic response of multilayer anisotropic pavements under simple harmonic loads. Verified through computer-aided methods, this approach proved effective for flexible pavement design. Wavelet analysis was also introduced to study three-dimensional frame structures and the dynamic response under vehicle loads. However, assuming equal interlayer adhesion coefficients in all directions exposes limitations in current analytical methods for flexible pavements.

In addition to indoor experimental studies, the finite element analysis (FEA) method has emerged as a crucial research tool, gaining recognition in engineering and academic circles. Sayyed et al. [24] conducted FEA of the optimal cross section for flexible pavements, referencing existing Indian standards and incorporating practical design methodologies. The research findings revealed that excessively soft asphalt mixtures can undermine pavement structural performance at high temperatures, while overly rigid asphalt mixtures may become brittle at low temperatures, leading to surface cracking under applied loads. By simulating actual wheel loads, Peng B et al. [25] examined the effects of a depleted asphalt macadam buffer layer on mitigating reflection cracks in semirigid bases. Their research concluded that this type of depleted asphalt macadam exhibits favorable pavement performance and is suitable for use as an antireflection buffer layer in semirigid bases. The use of a warm mix asphalt-modified mixture as a stress-absorbing layer to alleviate pavement reflection cracks was suggested by Pan R et al. [26], and its good anticracking effect was verified through FEA and indoor tests. These studies have revealed that the challenges associated with controlling indoor test conditions can be addressed through finite element software-based analyses of base structures, allowing for an intuitive understanding of performance changes through visualization techniques. However, the complexity of the software analysis process and the difficulties in accurate modeling still need to be resolved in future research.

Given the deficiencies in existing studies, this study investigates the reinforcement of flexible macadam bases using geogrids to enhance their bending fatigue performance. A composite base structure, consisting of a geogrid-reinforced macadam base and a cement-stabilized macadam base, was designed to mitigate reflection cracks in pavements. Indoor bending strength tests and three-point bending fatigue tests were conducted on both reinforced and unreinforced specimens under varying load levels. The results demonstrated that geogrid reinforcement significantly improved the bending performance and fatigue life of the macadam base, enhancing its dynamic stability under high-load conditions. This research provides a theoretical basis for the application of geogrid-based reinforcement in macadam base structures.

The remainder of this study is organized as follows: Section III provides a description of the comparative test profile for Macadam Bases. Section IV analyzes the test results regarding bending strength and crack resistance obtained from the comparative tests on macadam bases, categorized into Groups A and B. This section discusses the influence of different stress levels on bending strength as determined by the bending tensile test, as well as the effect of varying loading cycles on fatigue resistance from the three-point fatigue test. Section V summarizes the entire paper and presents the conclusions drawn from the findings.

3. METHODOLOGY

3.1. TEST CONDITIONS

In this study, the reinforced and unreinforced specimens, each measuring 150×150×550 mm, were subjected to comparative testing. Geogrids were placed between the cement-stabilized macadam base and the graded macadam base, with all structures having a uniform thickness of 50 mm. The aggregate gradations for the various specimen configurations are presented in Tables 1–3(see section: supplementary material).

Before specimens were prepared, compaction tests were conducted on the cement-stabilized macadam and graded macadam aggregates, ensuring they met the specified grading range. These tests determined the maximum dry density and optimum moisture content in the laboratory, with the results presented in Table 4(see section: supplementary material). The compaction curves for these aggregates are illustrated in Fig. 1(see section: supplementary material). For uniform distribution of aggregates, a rigid press block was placed above the aggregate during compaction. Pressure was applied using two large-tonnage jacks, which ensured stable pressure output throughout the loading process, as depicted in Fig. 3(see section: supplementary material). A total of 60 beam specimens were constructed using a wooden mold and evenly divided into Groups A and B based on the use of geogrids. Each group was subjected to five stress levels, with five specimens allocated to each level. All the prepared specimens were cured in a standard environmental chamber (temperature = 20°C ± 2°C, humidity ≥ 95%) for 90 days. The detailed parameters of the specimens are displayed in Fig. 2(see section: supplementary material).

3.2. TESTING EQUIPMENT AND LOADING SCHEME

In this experiment, all specimens underwent three-point bending load tests using an MTS 810 servo fatigue machine, as shown in Fig. 4(see section: supplementary material). During the loading process, the distance between the spherical movable supports was initially set to 300 mm. The specimen was then placed on the spherical movable support, and three points were marked for reference. Throughout compaction, the loading direction was maintained in alignment with the pressing direction. The upper and lower pressure heads were positioned at three specific locations on the specimen, as illustrated in Fig. 5(see section: supplementary material).

In the test, the fatigue load was applied using a Haversine cyclic variation mode at a loading frequency of 10 Hz. The loading waveform is shown in Fig. 6(see section: supplementary material). Prior to loading, a bending tensile strength test was conducted on the beams to determine the maximum bending strength of reinforced and unreinforced specimens. An appropriate stress loading level was then selected. During the fatigue loading phase, a pre-pressing procedure was implemented at 0.2 times the stress level to minimize the effects of poor contact. Subsequently, the stress was added based on design load until the specimen experienced complete compression failure.

In Fig. 6, P_{max} is the maximum load, P_{min} is the minimum load, $P_{min} = 0.02 \times P_{max}$, $P_0 = P_{max} - P_{min}$, T_0 is the loading cycle, and $T_0 = 1/f$ is the loading frequency (standard frequency: 10 Hz).

3.3. DATA ACQUISITION AND MEASUREMENT CONTENT

In this test, the data acquisition system consisted of a deformation-measuring instrument and a time recorder. The displacement measurement system was utilized to assess the bending deformation of the specimen, allowing for the determination of the load–deformation relationship during the bending process. The output load and loading cycles from the hydraulic servo were recorded by a computer for further analysis. In line with the test objectives, the measurement components included the following:

(1) Maximum bending strength of the specimen.

(2) Displacement of the specimen at top loading points.

(3) Under various stress conditions, the fatigue loading levels and loading cycles applied to the specimen.

4. RESULT ANALYSIS AND DISCUSSION

4.1. ANALYSIS OF FLEXURAL-TENSILE STRENGTH TEST RESULTS

4.1.1. GROUP A

Four bending tensile strength tests were conducted on unreinforced composite macadam base specimens (Group A). The displacement deformation yield curves for each test were obtained using the data acquisition system. Representative bending failure yield curves (Fig. 7) were identified through error analysis and processing of data.

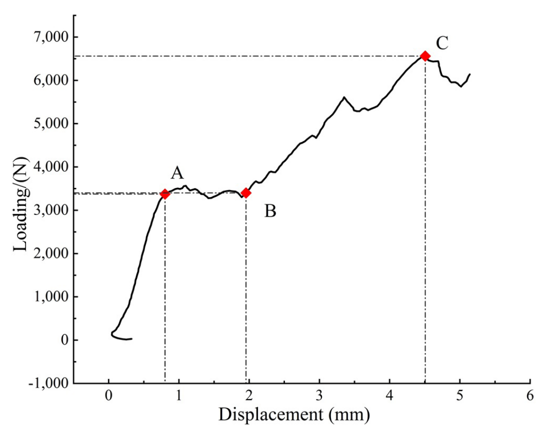

Fig. 7. Bending failure curves of the macadam base.

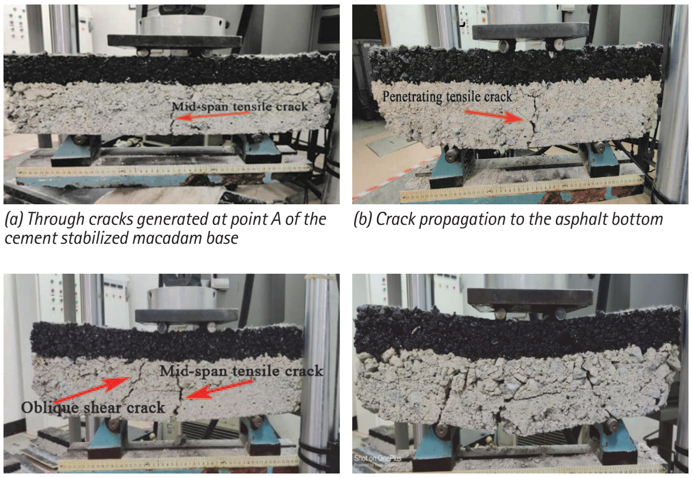

(a) Through cracks generated at point A of the cement stabilized macadam base *(b) Crack propagation to the asphalt bottom*

(c) Oblique shearing fracture of the specimen near the support in segment BC *(d) Bending failure of specimens*

Fig. 8. Bending failure of specimens

Fig. 7 shows that upon loading, the curve steadily ascended, indicating good stiffness and high bearing capacity of the cement-stabilized macadam base, with a gradual increase in displacement. At point A, through cracks began to form in the cement-stabilized base. In specimens without geogrids, transient cracks appeared when cracks developed under load, and these cracks propagated to the bottom of the asphalt layer. The bearing capacity in segment AB of the base decreased significantly, and macadam particles shifted under load, causing rapid displacement growth and widening of reflection cracks. After point B, the macadam aggregate rearranged, reaching a new dynamic equilibrium. Segment BC marked the asphalt pavement failure stage, where stress concentration was reduced by the loose structure near the support and macadam layer, lowering tensile stress in the sub-base. Diagonal shear cracks appeared in the cement-stabilized macadam base, and the asphalt layer underwent bending deformation, with displacement gradually increasing until failure. At point C, the bending tensile strength and displacement were 6.583 kN and 4.48 mm, respectively. The failure modes are shown in Fig. 8.

4.1.2. GROUP B

Through the same testing method as in Group A, the bending failure curves for the reinforced macadam base specimens in Group B were obtained. Fig. 9 shows that after geogrids were added, the overall failure curve of the specimen continuously rose at the same rate during the whole test process. Unlike the sharp increase in displacement observed in Figure 7, the bending tensile strength and displacement at point D reached 8.615 kN and 9.33 mm, respectively. This result indicated a notable improvement of 30.86% in bending tensile strength and a 108.25% increase in failure displacement compared with those of the unreinforced macadam base. Furthermore, the curve displayed a zigzag fluctuation near the failure point, indicating that as the specimen approached failure, the macadam base aggregates were further compacted because of the tensile action exerted by the geogrids.

Consequently, the macadam base regained its bearing capacity, allowing the specimen to undergo further bending deformation without sustaining damage. Overall failure of the specimen occurred only when the geogrids were fractured. The specific failure modes are illustrated in Fig. 10.

Fig. 10a illustrates that following the arrangement of geogrids, the macadam base could still separate through cracks from the cement-stabilized macadam base even cracks propagated. Consequently, the transmission of cracks directly transferred to the bottom of the asphalt surface course along the macadam base was significantly inhibited. With the gradual increase in displacement, geogrids were gradually stretched, thus enhancing the deformability of the specimen in the face of failure. As shown in Fig. 10b, geogrids effectively reduced the propagation of diagonal shear cracks near the support in case of specimen failure, evidenced by decreases in crack width and propagation speed. Hence, the overall bending resistance of the pavement structure was strengthened, and the propagation of reflection cracks was inhibited.

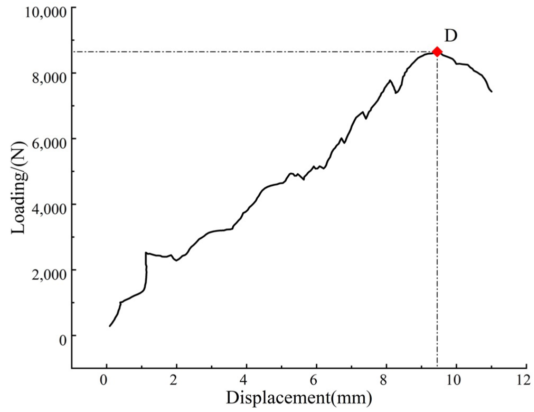

Fig. 9. Bending failure curves of reinforced macadam foundation

(a) Cut-through crack of the cement-stabilized macadam foundation of reinforced specimens *(b) Breakage failure of reinforced specimens*

Fig. 10. Bending failure curves of reinforced macadam foundation

Table 5(Supplementary material) and Fig. 11 show that at stress levels of 0.6 and 0.7, the reinforced specimens exhibited more fatigue cycles than the unreinforced ones, but the geogrids were not fully stretched, resulting in a small difference between the two groups. The reinforced specimens had an average fatigue life increase of 21.09%. At a stress level of 0.76, the fatigue life of unreinforced specimens dropped to one-quarter of that at 0.7, while the reinforced specimens retained 60% of their fatigue life, highlighting the poor dynamic stability of the macadam base under high stress. Once cracks formed in the cement-stabilized macadam base, the bearing capacity decreased significantly, and the loose base could not sustain long-term dynamic loads, leading to bending fatigue failure. The geogrid reinforcement improved the stability under dynamic loading, significantly extending the bending fatigue life of the pavement. This demonstrates that reinforcement enhances the bending fatigue performance of macadam base pavements.

4.2. THREE-POINT BENDING FATIGUE TEST ANALYSIS

In this test, five pressure levels were selected for both Groups A and B, with five specimens used for parallel testing at each stress level. Upon completion of the tests, measurement errors and average values of the five specimens were analyzed to reduce data variability. For each stress level, three datasets with similar characteristics were randomly chosen as representative data (Table 5). The fatigue loading cycles for Groups A and B across the different stress levels are illustrated in Fig. 11.

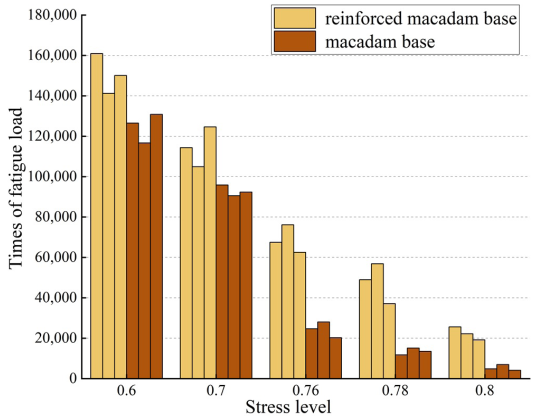

Fig. 11. Number of fatigue loading cycles under different stress levels

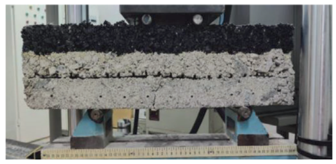

(a) 10,000 loading cycles

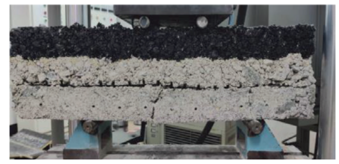

(b) 30,000 loading cycles

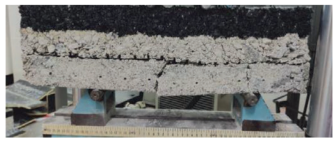

(c) 70,000 loading cycles

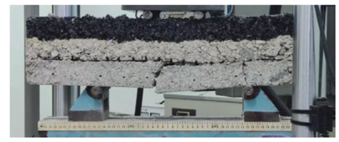

(d) 90,000 loading cycles

Fig. 13. Fatigue crack propagation on the reinforced macadam foundation

Fig. 11 shows that at a stress level of 0.8, the unreinforced macadam base failed due to low-cycle fatigue, while the reinforced macadam base maintained a high fatigue life of around 20,000 cycles. While the boundary between high- and low-cycle fatigue is not strict, low-cycle fatigue failure is typically defined by cycles that exceed the material's yield limit, leading to plastic deformation and macrocrack formation. Preventing low-cycle fatigue is essential for durable pavement structures. Geogrid reinforcement helped the macadam base maintain high-cycle fatigue resistance at 0.8 stress, reducing brittle failure and extending pavement fatigue life.

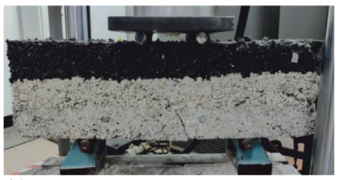

(a) 10,000 loading cycles

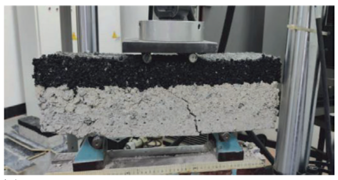

(b) 30,000 loading cycles

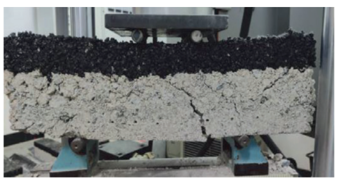

(c) 70,000 loading cycles

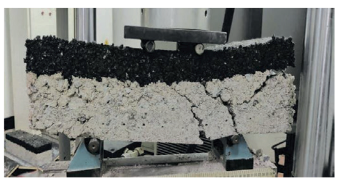

(d) 90,000 loading cycles

Fig. 12. Number of fatigues loading cycles under different stress levels

4.3. CRACK PROPAGATION AND COMPARATIVE TEST RESULTS

In the comparative test of crack propagation between reinforced and unreinforced specimens, a stress level of 0.7 was applied, and fatigue cracks were recorded at specific loading cycles, as shown in Fig. 12 and 13. Comparison of the crack propagation under different loading cycles in these figures indicated that in Group A, reflection cracks had already traversed the entire base structure by 30,000 cycles. At 70,000 cycles, distinct diagonal shear cracks formed along the edges of the macadam base and near the support. The specimens in Group A fractured completely after loading 90,000 cycles.

Severe bending deformation was observed in Group A's top asphalt layer, which detached from the macadam, causing significant damage. In contrast, Group B showed no reflection cracks through the entire base after 70,000 cycles. A crack was observed only in the cement-stabilized macadam base at midspan, but it did not propagate upward due to the geogrid's restraining effect. Shear fractures near the support in Group B were smaller than in Group A. After 90,000 cycles, the reflection crack in Group B had not spread to the macadam base, maintaining structural integrity. Throughout the test, Group B exhibited minimal bending deformation, while Group A showed noticeable fluctuations and fractures after 30,000 cycles. In conclusion, geogrid reinforcement effectively suppressed reflection crack propagation, reduced macadam base cracking, and delayed diagonal shear crack development.

4.4. YIELD CURVES UNDER DIFFERENT STRESS LEVLES

Fatigue failure curves for Groups A and B at different stress levels are shown in Fig. 14. Fig. 14a illustrates that at low stress levels, Group A specimens had failure displacements ranging from 4 to 8 mm. The graded macadam base could not resist tensile stress, causing the cement-stabilized macadam base to crack immediately, with the crack fully penetrating the base. The asphalt layer alone bore the load, potentially developing fatigue cracks after reaching a critical displacement, leading to rapid failure. As stress levels increased to 0.76 or higher, fatigue life decreased significantly, and failure displacement averaged 4–6 mm. The ultimate stress level for the macadam base pavement was identified as 0.7–0.76, where dynamic stability sharply declined, making the structure prone to brittle failure. The cement-stabilized macadam base failed in low-cycle brittle failure under high load, fully cracking before the surface load could dissipate, losing its functionality as a flexible base.

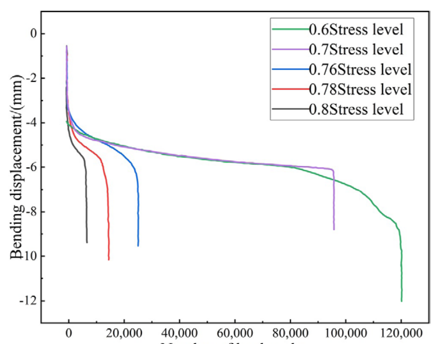

(a) Failure curve of Group A under different stress levels

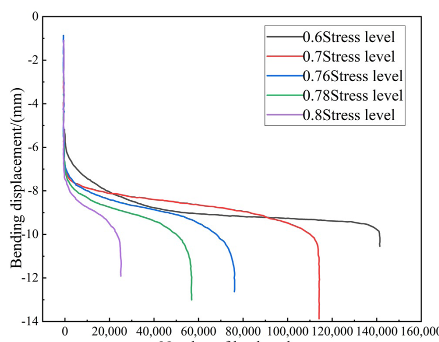

(b) Failure curve of Group B under different stress levels

Fig. 14. Failure curves under different stress levels

Fig. 14b demonstrates that at low stress levels, the displacement of the reinforced specimens at failure points ranged from 8 mm to 10 mm, approximately 50% higher than that of the unreinforced specimens. In the reinforced specimens, geogrids were tensioned as the specimens continued to undergo bending deformation, compacting and extruding the macadam aggregate. The load on the asphalt surface course was initially dispersed and attenuated by the macadam base. Subsequently, a portion of the remaining bending stress was converted into the frictional resistance at the geogrid–soil interface. Finally, the compressive stress transmitted to the cement-stabilized macadam base significantly declined; hence, the cement-stabilized macadam base could keep a relatively long fatigue life after through cracks formed. At stress levels exceeding 0.7, the failure curve did not attenuate significantly. At stress levels of 0.76 and 0.78, the reinforced specimens still exhibited large failure displacements. The macadam base could exert its pressure buffer effect to the greatest extent. This improvement in the antifatigue performance of the base structure under repeated vehicle loads effectively postponed pavement failure, enhanced the overall durability of the base, and extended the service life of the pavement.

5. ECONOMIC COMPARISON OF REINFORCED AND UNREINFORCED MACADAM BASE STRUCTURES

When comparing the economic aspects of reinforced and unreinforced macadam base structures, several factors such as initial construction costs, long-term maintenance expenses, service life, and social benefits must be considered. The following is a comprehensive analysis based on the research findings.

5.1. INITIAL CONSTRUCTION COSTS

Unreinforced macadam bases typically incur lower material costs and simpler construction processes, resulting in a reduced initial investment. In contrast, reinforced macadam bases require additional geogrid materials, which contribute 5%-15% of the total cost, along with the installation of geogrids during construction. This necessitates additional labor and equipment costs, leading to a higher initial cost for reinforced bases.

5.2. LONG-TERM MAINTENANCE AND REPAIR COSTS

Unreinforced bases are more susceptible to low-cycle fatigue failure under high stress, with cracks propagating rapidly. This results in frequent repairs, higher maintenance costs, and significant social costs due to traffic disruptions. Reinforced macadam bases, however, exhibit improved fatigue life, which delays crack propagation, reduces repair frequency, and consequently lowers long-term maintenance costs.

5.3. SERVICE LIFE AND LIFECYCLE COSTS

Unreinforced bases generally have a shorter service life and may require early reconstruction, increasing lifecycle costs. Reinforced bases, with improved dynamic stability, last 1.5 to 2 times longer, reducing the need for early reconstruction. Despite higher initial costs, reinforced bases often have lower overall lifecycle costs, especially for heavy-traffic roads.

5.4. INDIRECT ECONOMIC BENEFITS

Reinforced macadam bases suppress crack propagation, protecting upper layers and reducing maintenance. Their durability minimizes construction disruptions, improving service continuity and providing significant economic and social benefits. They are particularly beneficial for high-traffic roads or harsh environments, offering long-term returns.

Reinforced macadam bases provide clear long-term economic advantages, especially for high-durability, heavy-traffic roads. Despite the higher initial cost, their extended service life, reduced maintenance, and fewer reconstructions lead to lower lifecycle costs. Therefore, reinforced bases are recommended for long-term or high-traffic roads.

6. CONCLUSIONS

To address reflection cracks in traditional semirigid base structures, this study proposes a reinforced composite macadam base using geogrids between the macadam and cement-stabilized macadam layers to improve dynamic stability, bending performance, and fatigue life. Reinforced and unreinforced specimens underwent three-point bending fatigue and bending tensile tests to assess mechanical performance under five stress levels. Comparison of the results shows that geogrids significantly enhance the bending fatigue resistance of the macadam base. The main conclusions based on these findings are as follows:

(1) The macadam base alone cannot effectively inhibit reflection crack propagation. Once cracks reach the sub-base layer, they propagate to the asphalt surface. Geogrids, however, prevent vertical crack propagation, delaying diagonal shear crack formation near supports.

(2) The bending tensile test results show that the macadam base structure is prone to brittle failure under bending stress, with low failure displacement. Geogrid reinforcement improves bending strength and failure displacement by 30.86% and 108.25%, respectively, indicating enhanced resistance to bending deformation.

(3) The fatigue life of the macadam base is significantly reduced at stress levels above 0.7, with the ultimate stress between 0.7 and 0.76. Geogrids increase fatigue life across all stress levels and prevent rapid fatigue degradation, mitigating low-cycle fatigue failure at high stress levels and improving dynamic stability.

The reinforced macadam base offers ease of construction, cost-effectiveness, and high efficiency. Laboratory tests demonstrate superior bending strength, fatigue resistance, and dynamic stability under cyclic loading, making it a promising reinforcement solution for macadam bases in practical engineering. However, further research is needed to explore additional material parameters and improve the generalizability of the findings.

REFERENCES

[1] Zhou G, Li R, Wang H, et al. "Test on Performance of Reflective Cracking Resistance of Warp Knitting Fiberglass-polyester Paving Mat". China Journal of Highway and Transport. February 2016. Vol. 29-2. p.16-22. DOI: 1001-7372(2016)02-0016-07

[2] Tomás A, Olivares G. "Optimum reinforcement and sizing of concrete cross sections subjected to flexural and axial loading". DYNA. September 2018. Vol. 93-5. p.512-520. DOI: https://doi.org/10.6036/8676

[3] Xin Q, Dou Y, Zhang J, et al. "Deflection calculation of partially prestressed concrete beams under heavy duty". DYNA. March 2018. Vol. 93-3. p.301-307. DOI: https://doi.org/10.6036/8737

[4] Zhou L, Zheng M, Ma Q, et al. "Simulation of reflection crack propagation path for complex pavement with stress absorbing layer". Journal of Railway Science and Engineering. February 2016. Vol. 13-8. p.1507-1514. DOI: 1672-7029(2016)08-1507-08

[5] Harikumar M, Sankar N, Chandrakaran S. "Effect of Multi-Directional Reinforcements on the Settlement and Heave Characteristics of Foundations

on Sand". Geotechnical and Geological Engineering. August 2020. Vol. 42-8. p.827-837. DOI: https://doi.org/10.1007/s10706-020-01506-z
[6] Ouria A, Mahmoudi A, Sadeghpour H. "Effect of the Geotextile Arrangement on the Bearing Capacity of a Strip Footing". International Journal of Geosynthetics and Ground Engineering. August 2020. Vol. 6-36. p.1-14. DOI: https://doi.org/10.1007/s40891-020-00219-w
[7] Ban H, Im S. "Laboratory tests and finite element simulations to model thermally induced reflective cracking of composite pavements". International Journal of Pavement Engineering. January 2017. Vol. 19-3. p.220-230. DOI: https://doi.org/10.1080/10298436.2017.1279491
[8] Lu L, Zhang J, Ma S, et al. "Dynamic response of prestressed wrap-reinforced earth retaining walls". Chinese Journal of Geotechnical Engineering. February 2020. Vol. 42-2. p.344-353. DOI: https://doi.org/10.11779/CJGE202002016
[9] Liu M, Zhao X, Ge Z. "Design and Computational Method for Bridge Approach Reinforced Backfills". China Journal of Highway and Transport. May 2014. Vol. 27-2. p.17-26. DOI: https://doi.org/10.19721/j.cnki.1001-7372.2014.02.003
[10] Behnam M, Hashemolhosseini H, Mirmohamadsadeghi M. "Investigating the Effect of Geocell Changes on Slope Stability in Unsaturated Soil". Technical Gazette. March 2020. Vol. 14-1. p.66-75. DOI: https://doi.org/10.31803/tg-20190606115822
[11] Zhao M, Chen D, Liu M, et al. "Deformation analysis of geocell-reinforced body under embankment load considering soil arch effect". Chinese Journal of Geotechnical Engineering. April 2020. Vol. 42-4. p.601-609. DOI: https://doi.org/10.11779/CJGE202004001
[12] Zhou D, Ma Z, Liu L, et al. "Study on Fatigue Performance of In-service Asphalt Pavement Based on Full-scale Accelerated Loading Test". Journal of Highway and Transportation Research and Development. November 2024. Vol. 37-1. p.17-24. DOI: https://doi.org/10.3969/j.issn.1002-0268.2020.01.003
[13] Chen S, Zhang X, Meng S, et al. "Fatigue Damage in Asphalt Layer Based on ALF Accelerated Loading Test". Journal of Highway and Transportation Research and Development. February 2012. Vol. 29-1. p.18-22. DOI: https://doi.org/10.4028/www.scientific.net/AMR.255-260.3238
[14] Ji X, Zheng N, Hou Y, et al. "Application of asphalt mixture shear strength to evaluate pavement rutting with accelerated loading facility (ALF)". Construction and Building Materials. April 2013. Vol. 41. p.1-8. DOI: https://doi.org/10.1016/j.conbuildmat.2012.11.111
[15] Gonzalez-Torre I, Calzada-Perez M, Vega-Zamanillo A, et al. "Experimental study of the behavior of different geosynthetics as anti-reflective cracking systems using a combined-load fatigue test". Geotextiles and Geomembranes. August 2015. Vol. 43-4. p.345-350. DOI: https://doi.org/10.1016/j.geotexmem.2015.04.001
[16] Saha D, Mandal J. "Potential use of reinforced reclaimed asphalt pavement (RAP) and wet mix macadam (WMM) mixture in flexible pavement construction". International Journal of Pavement Research and Technology. March 2020. Vol. 13-4. p.352-360. DOI: https://doi.org/10.1007/s42947-020-0080-6
[17] Saride S, Kumar V. "Influence of geosynthetic-interlayers on the performance of asphalt overlays on pre-cracked pavements". Geotextiles and Geomembranes. January 2017. Vol. 45-3. p.184-196. DOI: https://doi.org/10.1016/j.geotexmem.2017.01.010
[18] Correia N, Zornberg J. "Mechanical response of flexible pavements enhanced with geogrid-reinforced asphalt overlays". Geosynthetics International. January 2016. Vol. 23-3. p.183-193. DOI: https://doi.org/10.1680/jgein.15.00041
[19] Hadi M, Al-Hedad A. "Flexural fatigue behavior of geogrid reinforced concrete pavements". Construction and Building Materials. July 2020. Vol. 249. p.1-10. DOI: https://doi.org/10.1016/j.conbuildmat.2020.118762
[20] Valli S, Kolathayar S. "Effect of Natural Rubber, Carbon Black, and Copper Slag as Construction Materials in Flexible Pavement: A Review". Advances in Transportation Engineering. May 2019. Vol. 34. p.59-64. DOI: https://doi.org/10.1007/978-981-13-7162-2_6
[21] Patil V, Joshi P, Kale S, et al. "Design of Flexible Pavement on Black Cotton Soil Stabilized with RBI Grade 81". Environmental Geotechnology. May 2019. Vol. 31. p.193-200. DOI: https://doi.org/10.1007/978-981-13-7010-6_18
[22] Habbouche J, Hajj E, Morian N. "Reflective cracking relief interlayer for asphalt pavement rehabilitation: from development to demonstration". Road Materials and Pavement Design. October 2017. Vol. 18-4. p.30-57. DOI: https://doi.org/10.1080/14680629.2017.1389080
[23] You L, Man J, Yan K, et al. "Combined Fourier-wavelet transforms for studying dynamic response of anisotropic multi-layered flexible pavement with linear-gradual interlayers". Applied Mathematical Modelling. May 2020. Vol. 81. p.559-581. DOI: https://doi.org/10.1016/j.apm.2020.01.031
[24] Sayyed S, Patil R, Tapase A, et al. "Review and assessment of flexible pavement". Confronting Severe Weathers and Climate Changes Conference. July 2018. Vol. SUCI. p.139-149. DOI: https://doi.org/10.1007/978-3-319-96241-2_12
[25] Peng B, Tong X, Cao N, et al. "Research on anti-cracking and road performance of lean asphalt gravel intermediate structural Layer". Journal of Dalian University of Technology. July 2018. Vol. 54-4. p.385-391. DOI: https://doi.org/10.7511/dllgxb201804008
[26] Pan R, Cheng P. "Grading design and road use performance of warm mix rubber asphalt mixture suitable for stress absorbing layer in cold region". Buildings. November 2024. Vol. 14-12. p.3817. DOI: https://doi.org/10.3390/buildings14123817

SUPPLEMENTARY MATERIAL

https://www.revistadyna.com/documentos/pdfs/_adic/11402-1_en.pdf